



UDC 539.217

<https://doi.org/10.17073/1997-308X-2024-6-56-64>

Research article  
Научная статья



# The influence of porogen dispersion on the structure and permeability of highly porous material from nickel nanopowder

V. S. Shustov , V. A. Zelensky, M. I. Alymov,  
A. B. Ankudinov, A. S. Ustyukhin

A.A. Baikov Institute of Metallurgy and Materials Science of the Russian Academy of Sciences  
49 Leninskiy Prosp., Moscow 119334, Russia

 [vshscience@mail.ru](mailto:vshscience@mail.ru)

**Abstract.** The study investigates the structure, porosity, and permeability of highly porous materials based on nickel nanopowders, which were synthesized using ammonium carbonate as a porogen. The process of sample fabrication involves three technological steps: preparation of the initial mixtures of metal nanopowder with a porogen, compaction of the green samples, and subsequent sintering. The average particle size of the nickel powder was less than 100 nm. Ammonium carbonate powders with particle sizes of 40–63, 100–160, 200–250, and 315–400  $\mu\text{m}$ , obtained by sieving, were selected for the experiments. The porogen's volume fraction in the initial mixtures with nickel nanopowder was 60, 80, 85, and 88 %, with a compaction pressure of 300 MPa. The stages of sintering the nickel nanopowder were preceded by the removal of ammonium carbonate from the green sample by heating it in an argon flow to 100  $^{\circ}\text{C}$  at a rate not exceeding 1  $^{\circ}\text{C}/\text{min}$ . The optimal sintering temperature and time for the nickel nanopowder were determined to be 550  $^{\circ}\text{C}$  for 120 min. The research aimed to establish the influence of the porogen's particle size, its size distribution, and volume fraction on the material's porosity and permeability. The results showed that increasing the particle size and volume fraction of the porogen leads to higher porosity and permeability of the material. The maximum permeability value achieved was  $8.4 \cdot 10^{-12} \text{ m}^2$  from a sample with 88.5 % porosity, produced using a porogen with a particle size of 315–400  $\mu\text{m}$ . When using porogen powders with two different particle size ranges: 40–50  $\mu\text{m}$  and 315–400  $\mu\text{m}$  (or 100–125  $\mu\text{m}$  and 315–400  $\mu\text{m}$ ), the permeability was limited to values obtained from samples using only one of these fractions. In this case, the permeability changed nonlinearly depending on the ratio of each fraction component.

**Keywords:** permeability, porous material, nanopowder, nickel, ammonium carbonate

**Acknowledgements:** The work was completed according to state order № 075-00320-24-00.

**For citation:** Shustov V.S., Zelensky V.A., Alymov M.I., Ankudinov A.B., Ustyukhin A.S. The influence of porogen dispersion on the structure and permeability of highly porous material from nickel nanopowder. *Powder Metallurgy and Functional Coatings*. 2024;18(6):56–64. <https://doi.org/10.17073/1997-308X-2024-6-56-64>

# Влияние дисперсности порообразователя на структуру и проницаемость высокопористого материала из нанопорошка никеля

В. С. Шустов , В. А. Зеленский, М. И. Алымов,  
А. Б. Анкудинов, А. С. Устюхин

Институт металлургии и материаловедения им. А.А. Байкова Российской академии наук  
Россия, 119334, г. Москва, Ленинский пр-т, 49

 vshscience@mail.ru

**Аннотация.** В работе исследованы структура, пористость и проницаемость высокопористых материалов на основе нанопорошков никеля, полученных с использованием карбоната аммония в качестве порообразователя. Процесс изготовления образцов включает три технологические операции: приготовление исходных смесей нанопорошка металла с порообразователем, прессование заготовок и их спекание. Средний размер частиц порошка никеля составлял менее 100 нм. Для исследований выбраны порошки карбоната аммония с частицами размером 40–63, 100–160, 200–250 и 315–400 мкм, полученные методом ситового просева. Объемная доля порообразователя в исходных смесях с нанопорошком никеля составляла 60, 80, 85 и 88 %, давление прессования – 300 МПа. Стадии спекания нанопорошка никеля предшествовала стадия удаления карбоната аммония из прессовки путем ее нагревания в потоке аргона до температуры 100 °С со скоростью, не превышающей 1 °С/мин. Для нанопорошка никеля установлены рациональные значения температуры и времени спекания – 550 °С, 120 мин. Исследование направлено на установление влияния размера частиц порообразователя, их распределения по размеру и его объемной доли на пористость и проницаемость материала. Полученные результаты показали, что увеличение размера частиц порообразователя и его объемной доли приводит к повышению пористости и проницаемости материала. Максимальное значение достигнутой проницаемости составило  $8,4 \cdot 10^{-12}$  м<sup>2</sup> у образца с пористостью 88,5 %, полученного с применением порообразователя с размером частиц 315–400 мкм. При использовании порошков порообразователя с частицами сразу двух размерных диапазонов: 40–50 и 315–400 мкм (либо 100–125 и 315–400 мкм), проницаемость ограничивается значениями, полученными на образцах с применением порошка только одной из указанных фракций. При этом проницаемость меняется нелинейно в зависимости от соотношения каждой составляющей фракции.

**Ключевые слова:** проницаемость, пористый материал, нанопорошок, никель, карбонат аммония

**Благодарности:** Работа выполнена в рамках госзадания № 075-00320-24-00.

**Для цитирования:** Шустов В.С., Зеленский В.А., Алымов М.И., Анкудинов А.Б., Устюхин А.С. Влияние дисперсности порообразователя на структуру и проницаемость высокопористого материала из нанопорошка никеля. *Известия вузов. Порошковая металлургия и функциональные покрытия*. 2024;18(6):56–64. <https://doi.org/10.17073/1997-308X-2024-6-56-64>

## Introduction

Porous materials are used in many industries. The porous structure, typically regarded as a defect in structural materials, provides unique properties that can be utilized for specific purposes [1]. Highly porous materials can be effectively used as electrodes [2], filters that separate impurity particles larger than the pore size [3–5], and are often employed as thermal insulators [6; 7]. Another application of porous materials is in biocompatible implants [8]. The relatively high internal surface area makes highly porous materials excellent catalysts [9; 10].

Depending on the specific application and the required porous structure, various fabrication methods can be employed to produce such materials, including partial sintering, the use of temporary porogens, direct foaming, and others. In the first case, the powder material is sintered in such a way that pores remain between

the particles [11; 12]. This is due either to too low temperature and duration of sintering or to the low density of the initial green sample. In the second method, the added porogens decompose into volatile components or are washed out of the material during its production. The porous structure is controlled by appropriately selecting the porogenic substances. For porous materials produced using dispersed porogens, the shape and size of the pores depend on the shape and size of the porogen particles, while porosity is controlled by the quantitative content of the porogen [13]. This methodology allows for higher porosity values compared to the partial sintering technique. The approaches applied to the fabrication of highly porous materials from powders of various natures with the addition of temporary porogens are seen by the authors as promising, as they enable wide-ranging control over porosity and pore size in the resulting material.

It is important to note that simply having a highly porous structure is insufficient for certain applications. For filters and catalysts, it is necessary to create a porous material with a high proportion of open interconnected pores. This ensures good permeability, an important property for ensuring the reliable operation of the products in which they are used. Permeability is defined as the coefficient that relates the pressure gradient to the flow rate of the medium passing through the sample. It depends on the porous structure and can vary sharply with changes in the pore size distribution or the spatial arrangement and shape of the pore channels [10; 14–17]. It should be noted that a high porosity value does not always indicate good permeability.

In many studies where the authors create a porous material and investigate its structure, insufficient attention is paid to this parameter. However, some researchers provide permeability data without a thorough analysis of their relationship with the morphology of the porous space. Most studies focusing on permeability examine the flow of media through porous structures governed by Darcy's law or Forchheimer's law [18–25]. These laws are phenomenological and do not contain any condition describing the influence of the material's microstructure. Therefore, researchers face the pressing task of finding ways to accurately assess permeability based on models developed considering the material's microstructure parameters and allowing for predictions of permeability levels [26; 27]. Existing models do not fully account for all the features of the porous structures of modern materials, and creating new models requires a significant amount of experimental data on the relationship between permeability and various structural characteristics. Consequently, to better understand the processes, experimental studies are necessary to identify the connection between the structural features of the porous material and its permeability.

The aim of this work was to establish the influence of the porogen particle size and its volume fraction on the porosity and permeability of the nickel nanopowder material produced through pressing and sintering.

## Research methodology

Nickel nanopowder with an average particle size of less than 100 nm, produced by wire explosion technology, was used as the starting material for the production of porous samples. This powder contained a small amount of larger spherical particles, up to 3  $\mu\text{m}$  in size, which is a characteristic and drawback of this method for obtaining nanopowders. Ammonium carbonate  $(\text{NH}_4)_2\text{CO}_3$  powders were used as the porogen. To study the influence of the volume fraction and dis-

persion of the porogen on the structure and permeability, ammonium carbonate powders with particle sizes of  $d = 40\div 63$ ,  $100\div 160$ ,  $200\div 250$ , and  $315\div 400 \mu\text{m}$  were selected.

To determine the effect of the particle size distribution of the porogen on the structure and permeability, additional mixtures of the porogen were prepared, using particles from two size ranges:  $40\text{--}50$  and  $315\text{--}400 \mu\text{m}$ , as well as  $100\text{--}125$  and  $315\text{--}400 \mu\text{m}$ . For simplicity, these porogen powders will hereafter be referred to as "bidisperse". In each mixture, the amounts of both fractions of the powders were varied in steps of 25 % – from 100 % content of the powder with  $d = 40\div 50 \mu\text{m}$  (or  $100\div 125 \mu\text{m}$ ) to 100 % content of the powder with  $d = 315\div 400 \mu\text{m}$ .

The production of porous nickel materials consisted of three technological operations: preparing the initial mixtures of nickel nanopowder with the porogen, compacting the green samples, and sintering them. The volume fraction of the porogen in the initial mixtures was 60, 80, 85, and 88 %, with a compaction pressure of 300 MPa. The samples were produced by uniaxial compaction on a hydraulic press (Knuth, Germany) in a split mold with a diameter of 13.6 mm. The height of the compacts before sintering was 10 mm. To remove ammonium carbonate, the compacts were heated in an argon flow to a temperature of 100  $^\circ\text{C}$  at a rate not exceeding 1  $^\circ\text{C}/\text{min}$ . The optimal sintering temperature for the nickel nanopowder was determined to be 550  $^\circ\text{C}$ , with a sintering time of 120 min. The heating rate to the sintering temperature did not exceed 2  $^\circ\text{C}/\text{min}$ , which was necessary for the slow removal of the decomposition products of the porogen. Higher heating rates resulted in structural defects in the samples, such as microcracks. The thermal treatment of the samples was conducted in a tube furnace (MTI GSL1500X, USA).

Porosity was measured using the hydrostatic weighing method, with a relative error not exceeding 0.6 %. The permeability of the obtained porous nickel samples was determined using a method based on Darcy's law. For this, while a liquid flowed through the sample, the pressure drop across its ends and the flow rate of the liquid – determined by the known volume of liquid passing through the sample over a fixed period – were recorded. The study was conducted by passing distilled water under pressure at room temperature. The pressure drop across the tested samples varied from 0 to 0.02 MPa, with the value recorded using a digital manometer (DM5002M, Manotomy JSC, Russia) with an allowable measurement error of  $2 \cdot 10^{-5}$  MPa. The relative error in the permeability measurement did not exceed 10 %.

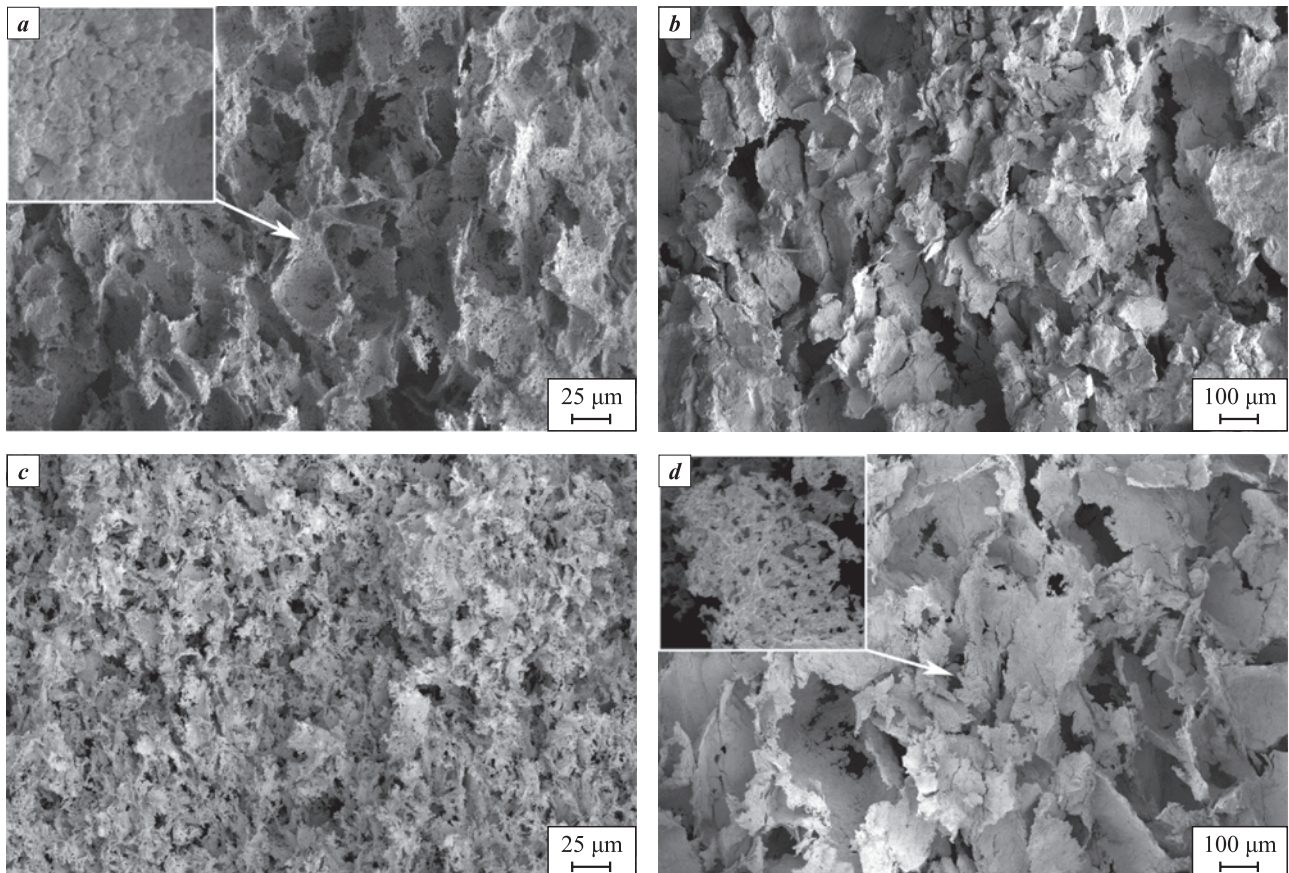
## Results and discussion

Fig. 1 presents the microstructure of the fracture surfaces of samples with porosities of 79.3 and 88.5 %, sintered in a hydrogen atmosphere at a temperature of 550 °C. The volume fraction of the porogen in the mixture from which these samples were pressed was 80 and 88 %, respectively. Scanning electron microscopy revealed that, due to the thermal decomposition of the porogen, a pore structure was formed, which can be considered a replica of the removed porogen, with some modification in their shape and size as a result of compaction and sintering. Due to the high activity of the nanopowders, sintering was conducted at a relatively low temperature, resulting in samples with sufficient strength necessary for further investigation of their permeability.

In samples with an initial porogen content of 88 %, a significant number of thin walls, with a thickness of no more than 1–3 μm, were observed, featuring “windows” formed at the points of contact between porogen particles as well as from the escape of decomposition products. The small amount of nickel powder

present in the framework of the highly porous material apparently defined a “lace-like” structure in these walls, characterized by numerous smaller holes or voids compared to the windows. Moreover, the smaller the porogen used, the more pronounced this structure became.

The influence of the volume fraction of the porogen and its dispersion on the porosity ( $P$ ) and permeability ( $K$ ) of the sintered material was investigated. Fig. 2 presents the dependencies of the porosity of the sintered material on the particle size ( $d$ ) of the porogen for samples in which the volume fraction of the porogen was 65, 80, 85, and 88 %. It is evident that the value of  $P$  increases with increasing values of  $d$ . When using a porogen with  $d > 100 \mu\text{m}$ , the porosity of the sintered material equals or exceeds the expected value, which is equal to the volume fraction of the porogen in the initial mixture. For  $d = 40\div 63 \mu\text{m}$ , the value of  $P$  was lower than expected, except for samples with a porogen volume fraction of 65 %. The closed porosity of all materials did not exceed 1 %. The porogen  $(\text{NH}_4)_2\text{CO}_3$  decomposes during sintering at temperatures below 100 °C. This leads to the release of pore space and



**Fig. 1.** SEM images of the fracture of nickel nanopowder samples obtained using a porogen of 80 vol. % (*a, b*) and 88 vol. % (*c, d*), and particle sizes of 40–63 μm (*a, c*) and 315–400 μm (*b, d*)

**Рис. 1.** РЭМ-изображения излома образцов из нанопорошка никеля, полученных с применением порообразователя объемной долей 80 % (*a, b*) и 88 % (*c, d*) и размером частиц 40–63 мкм (*a, c*) и 315–400 мкм (*b, d*)

the formation of channels that connect the pores to the free surface of the sample. The interconnection of pores in such materials determines the high proportion of open porosity and their permeability.

The dependence of permeability on the volume fraction of the porogen and its dispersion was inves-

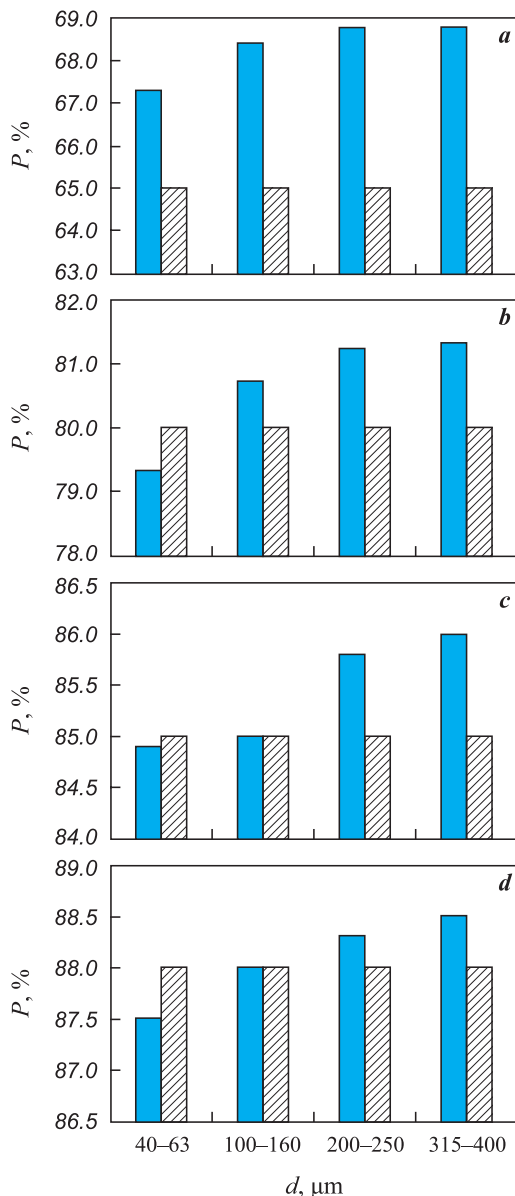


Fig. 2. Diagrams showing the dependence of the porosity of the sintered material on the particle size of the porogen for samples with volume fractions of 65 (a), 80 (b), 85 (c), and 88 % (d)

The hatching indicates the volume fraction of the porogen in the initial mixture

Рис. 2. Диаграммы зависимости пористости спеченного материала от размера частиц порообразователя для образцов, в которых объемная доля последнего составляла 65 (а), 80 (б), 85 (с) и 88 % (д)

Штриховкой указана объемная доля порообразователя в исходной смеси

tigated (Fig. 3). It was found that as the volume fraction of the porogen increases, the permeability also rises. Additionally, this increase is achieved through the enlargement of the porogen particle size while maintaining a constant volume fraction in the initial powder mixture. For example, with a porogen content of 65 vol. %, the permeability ( $K$ ,  $10^{-12}$ ) increases from 0.1 to 0.4  $m^2$ , at 80 vol. %, it rises from 1 to 2.9  $m^2$ , at 85 vol. %, from 1.8 to 4.6  $m^2$ , and at 88 vol. %, from 3.9 to 8.4  $m^2$ .

Fig. 4 illustrates the dependence of permeability on the porosity of the material for samples obtained using porogen powder with particles of a specified size range.

Using the compaction and sintering regimes described above, samples were obtained from mixtures of nickel nanopowder and bidisperse porogen, with the latter fixed at 85 vol. %. Data from Fig. 5 show that the samples contain pores corresponding to the sizes of the particles of the porogen used – large pores from particles with diameters of 315–400  $\mu m$  and small pores from particles with diameters of 40–50  $\mu m$  or 100–125  $\mu m$  (Fig. 5, a, b). No inhomogeneity in the pore distribution within the volume of the samples was detected.

It is noteworthy that in samples containing the porogen with smaller particle sizes (40–50  $\mu m$ ), there was a greater number of windows on the surfaces of the larger pores. These windows are comparable in size to the smaller porogen particles and were likely formed due to their contact with the larger ones. It can be hypothesized that a greater number of windows will provide better permeability in this series of samples, along with the high permeability achieved

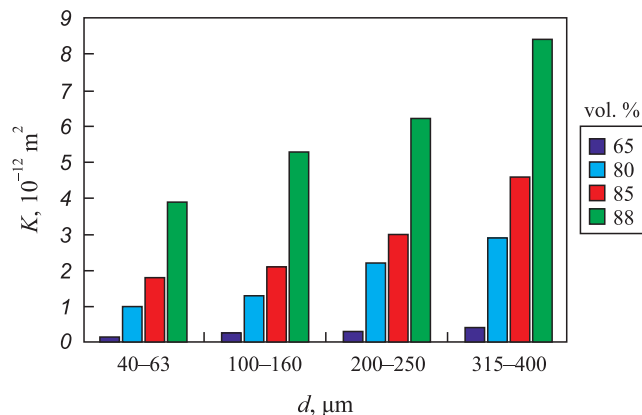
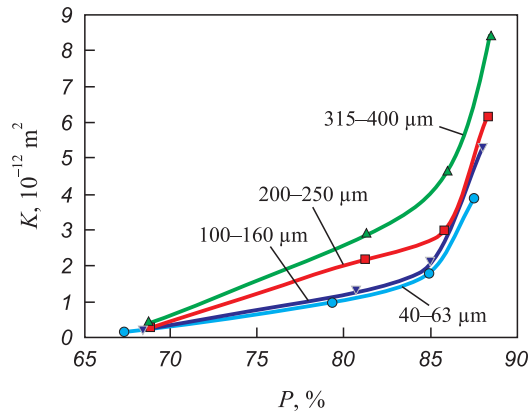


Fig. 3. Diagram showing the dependence of the permeability of the nickel nanopowder material on the volume fraction of the porogen and its dispersion

Рис. 3. Диаграмма зависимости проницаемости материала из нанопорошка никеля от объемной доли порообразователя и его дисперсности



**Fig. 4.** Graph showing the dependence of the material's permeability on the total porosity for samples obtained using porogens of varying dispersion

**Рис. 4.** График зависимости проницаемости материала от общей пористости для образцов, полученных с применением порообразователей разной дисперсности

by using porogen with particle sizes of 315–400 μm. However, according to the results of the study (Fig. 6), the samples obtained from mixtures with smaller poro-

gen particles (40–50 μm) exhibited lower permeability compared to those using powders with diameters of 100–125 μm. The content of larger porogen particles (315–400 μm) ranging from 0 to 50 % did not lead to a significant change in the value of  $K$ : for samples made with porogen of 40–50 μm, the permeability was  $(1.3 \pm 0.1) \cdot 10^{-12} \text{ m}^2$ , while with 100–125 μm it was  $(2.2 \pm 0.2) \cdot 10^{-12} \text{ m}^2$ . Further increasing the proportion of 315–400 μm particles in the porogen resulted in an increase in  $K$  to  $4.6 \cdot 10^{-12} \text{ m}^2$ .

## Conclusions

As a result of the conducted studies on the structure and permeability of the obtained porous materials, the following conclusions were established.

1. The permeability of highly porous materials made from nickel nanopowders increases with both the volume fraction of the porogen, ranging from 60 to 88 %, and the particle size of the porogen. The maximum permeability achieved was  $8.4 \cdot 10^{-12} \text{ m}^2$  in a sample with a porosity of 88.5 %.

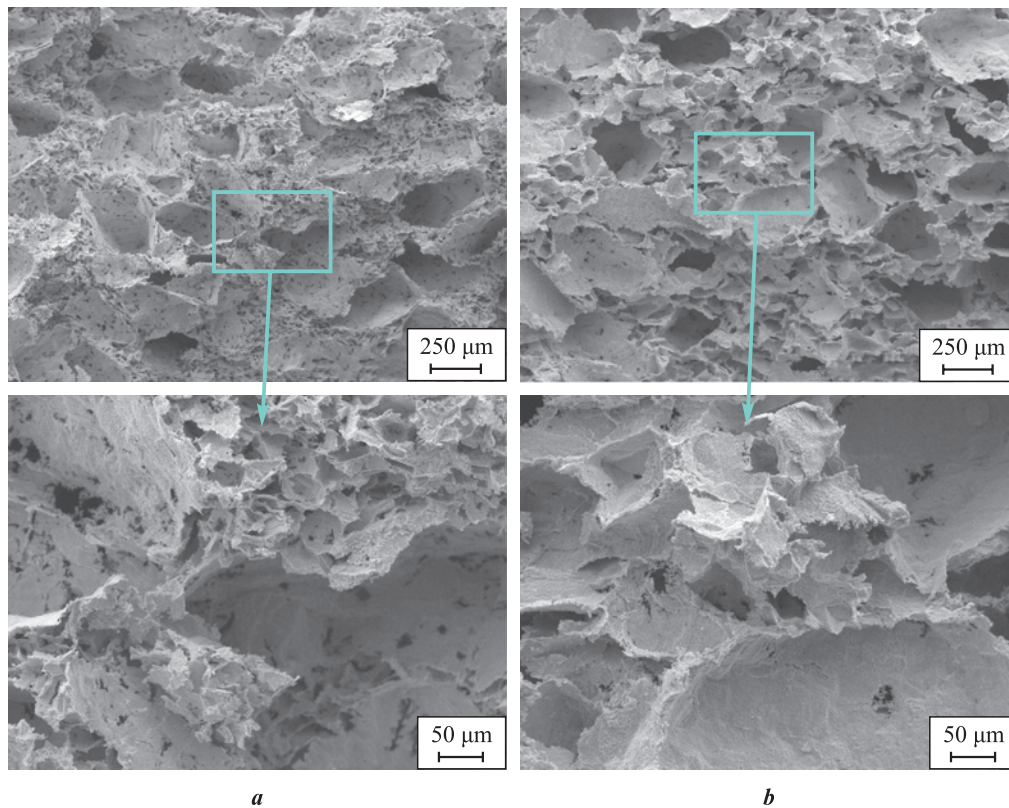


**Fig. 5.** SEM images of the fracture of porous nickel nanopowder samples obtained using a bidisperse porogen with particle sizes of 40–50 and 315–400 μm (a), and 100–125 and 315–400 μm (b)

The volume ratio of porogen particles of both sizes in the samples was 50:50

**Рис. 5.** РЭМ-изображения излома пористых образцов из нанопорошка никеля, полученных с применением бидисперсного порообразователя с размером частиц 40–50 и 315–400 мкм (a) и 100–125 и 315–400 мкм (b)

Объемное соотношение частиц порообразователя обоих размеров в образцах составляло 50:50

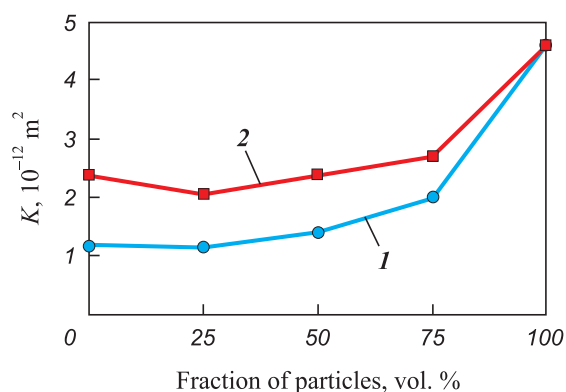


**Fig. 6.** Dependence of the permeability of samples obtained using a bidisperse porogen on the volume fraction of particles sized 315–400  $\mu\text{m}$  in the initial mixture containing particles sized 40–50  $\mu\text{m}$  (1) and 100–125  $\mu\text{m}$  (2)

**Рис. 6.** Зависимость проницаемости образцов, полученных с применением бидисперсного порообразователя, от объемной доли его частиц размером 315–400 мкм в исходной смеси дисперсностью 40–50 мкм (1) и 100–125 мкм (2)

2. Using a bidisperse porogen facilitates smoother regulation of the permeability in nickel nanopowder materials. As the proportion of larger particles (315–400  $\mu\text{m}$ ) in the porogen powder increases, the samples exhibit enhanced permeability. The lowest permeability was recorded when only fine porogen was used (e.g., with particle sizes of 40–50  $\mu\text{m}$  or 100–125  $\mu\text{m}$ ). When up to 50 vol. % of larger particles is added, the permeability varies by approximately 10 %. A notable increase in permeability, reaching  $4.6 \cdot 10^{-12} \text{ m}^2$ , is observed at a 100 % volume fraction of porogen particles sized 315–400  $\mu\text{m}$  in the initial mixture.

## References / Список литературы

- Lefebvre L., Banhart J., Dunand D.C. Porous metals and metallic foams: Current status and recent developments. *Advanced Engineering Materials*. 2008;10(9):775–787. <https://doi.org/10.1002/adem.200800241>
- Chen H., Hu L., Chen M., Yan Y., Wu L. Nickel-cobalt layered double hydroxide nanosheets for high – performance supercapacitor electrode materials. *Advanced Functional Materials*. 2014;24(7):934–942. <https://doi.org/10.1002/adfm.201301747>
- Maggay I.V., Chang Y., Venault A., Dizon G.V., Wu C.J. Functionalized porous filtration media for gravity-driven filtration: Reviewing a new emerging approach for oil and water emulsions separation. *Separation and Purification Technology*. 2021;259:117983. <https://doi.org/10.1016/j.seppur.2020.117983>
- Mazurkow J.M., Yüzbaşı N.S., Domagala K.W., Pfeiffer S., Kata D., Graule T. Nano-sized copper (oxide) on alumina granules for water filtration: effect of copper oxidation state on virus removal performance. *Environmental Science & Technology*. 2019;54(2):1214–1222. <https://doi.org/10.1021/acs.est.9b05211>
- Hellmann A., Pitz M., Schmidt K., Haller F., Ripberger S. Characterization of an open-pored nickel foam with respect to aerosol filtration efficiency by means of measurement and simulation. *Aerosol Science and Technology*. 2015;49(1):16–23. <https://doi.org/10.1080/02786826.2014.990555>
- Qiu L., Zou H., Tang D., Wen D., Feng Y., Zhang X. Inhomogeneity in pore size appreciably lowering thermal conductivity for porous thermal insulators. *Applied Thermal Engineering*. 2018;130:1004–1011. <https://doi.org/10.1016/J.APPLTHERMALENG.2017.11.066>
- Jia C., Li L., Liu Y., Fang B., Ding H., Song J., Liu Y., Xiang K., Lin S., Li Z., Si W., Li B., Sheng X., Wang D., Wei X., Wu H. Highly compressible and anisotropic lamellar ceramic sponges with superior thermal insulation and acoustic absorption performances. *Nature Communications*. 2020;11(1):1–13. <https://doi.org/10.1038/s41467-020-17533-6>
- Szłazak K., Jaroszewicz J., Ostrowska B., Jaroszewicz T., Nabilek M., Szota M., Swieszkowski W. Characterization of three-dimensional printed composite scaffolds prepared with different fabrication methods. *Archives of Metallurgy and Materials*. 2016;61(2A):645–650. <https://doi.org/10.1515/amm-2016-0110>
- Yang C., Zhang C., Chen Z. J., Li Y., Yan W.Y., Yu H.B., Liu L. Three-dimensional hierarchical porous structures of metallic glass/copper composite catalysts by 3D printing for efficient wastewater treatments. *ACS Applied Materials & Interfaces*. 2021;13(6):7227–7237. <https://doi.org/10.1021/acsami.0c20832>
- Ibrahim S.H., Skibinski J., Oliver G.J., Wejrzanowski T. Microstructure effect on the permeability of the tape-cast open-porous materials. *Materials and Design*. 2019;167:1–7. <https://doi.org/10.1016/j.matdes.2019.107639>
- Ohji T., Fukushima M. Macro-porous ceramics: processing and properties macro-porous ceramics: processing and properties. *International Materials Reviews*. 2013;57(2):115–131. <https://doi.org/10.1179/1743280411Y.0000000006>
- Lyckfeldt O., Ferreira J.M.F. Processing of porous ceramics by ‘starch consolidation’. *Journal of the European Ceramic Society*. 1998;18(2):131–140. [https://doi.org/10.1016/S0955-2219\(97\)00101-5](https://doi.org/10.1016/S0955-2219(97)00101-5)
- Li Y., Yang X., Liu D., Chen J., Zhang D., Wu Z. Permeability of the porous  $\text{Al}_2\text{O}_3$  ceramic with bimodal pore size distribution. *Ceramics International*. 2019;45(5):5952–5957. <https://doi.org/10.1016/j.ceramint.2018.12.064>
- Lv C., Li W., Du J., Liang J., Yang H., Zhu Y., Ma B. Experimental investigation of permeability and Darcy-Forchheimer flow transition in metal foam with high pore density. *Experimental Thermal and Fluid Science*. 2024;154:111149. <https://doi.org/10.1016/j.expthermflusci.2024.111149>
- Afsharpoor A., Javadpour F. Liquid slip flow in a network of shale noncircular nanopores. *Fuel*. 2016;180:580–590. <https://doi.org/10.1016/j.fuel.2016.04.078>
- Xu X., Liu X., Wu J., Zhang C., Tian K., Yu J. Effect of preparation conditions on gas permeability parameters

- of porous SiC ceramics. *Journal of the European Ceramic Society*. 2021;41(6):3252–3263.  
<https://doi.org/10.1016/j.jeurceramsoc.2021.01.015>
17. Dai Q., Wang G., Zhao X., Han Z., Lu K., Lai J., Wang S., Li D., Li Y., Wu K. Fractal model for permeability estimation in low-permeable porous media with variable pore sizes and unevenly adsorbed water lay. *Marine and Petroleum Geology*. 2021;130:105135.  
<https://doi.org/10.1016/j.marpetgeo.2021.105135>
  18. Dukhan N., Bağcı Ö., Özdemir M. Metal foam hydrodynamics: Flow regimes from pre-Darcy to turbulent. *International Journal of Heat and Mass Transfer*. 2014;77:114–123.  
<https://doi.org/10.1016/j.ijheatmasstransfer.2014.05.017>
  19. Belyaev E.S., Khlybov A.A., Matsulevich Z.V., Titov E.Y., Getmanovsky Y.A., Belyaeva S. S., Bystrov E.O., Ryabov D.A., Kovylin R.S., Tchesnokov S.A., Bazanov A.V., Mezhevoi I.N., Baykov V.E., Yunin V.V. Micromechanics of porosity of various degrees in porous permeable Ti–V30 getter made of powder. *Vacuum*. 2023;211:111934.  
<https://doi.org/10.1016/j.vacuum.2023.111934>
  20. Tang H.P., Wang J., Qian M. 28-Porous titanium structures and applications. In: *Titanium Powder Metallurgy*. Ed. Ma Qian, Francis H. (Sam) Froes, Butterworth-Heinemann, 2015. P. 533–554.  
<https://doi.org/10.1016/B978-0-12-800054-0.00028-9>
  21. Xie D., Dittmeyer R. Correlations of laser scanning parameters and porous structure properties of permeable materials made by laser-beam powder-bed fusion. *Additive Manufacturing*. 2021;47:102261.  
<https://doi.org/10.1016/j.addma.2021.102261>
  22. Lupo M., Neveu A., Gemine T., Francqui F., Lumay G. Measuring permeability and flowability of powders at various packing fractions. *Particuology*. 2024.  
<https://doi.org/10.1016/j.partic.2024.03.008>
  23. Xu Y., Zhang S., Ding W., Du H., Li M., Li Z., Chen M. Additively-manufactured gradient porous bio-scaffolds: Permeability, cytocompatibility and mechanical properties. *Composite Structures*. 2024;336:118021.  
<https://doi.org/10.1016/j.compstruct.2024.118021>
  24. Li C., Zhou Z. Preparation and characterization of permeability and mechanical properties of three-dimensional porous stainless steel. *RSC Advances*. 2022;12(43):28079–28087. <https://doi.org/10.1039/D2RA03893E>
  25. Sauermoser-Yri M., Veldurthi N., Wölflé C.H., Svartvatn P.J., Hoem S.O.F., Lid M.J., Bock R., Palko J.W., Torgersen J. On the porosity-dependent permeability and conductivity of triply periodic minimal surface based porous media. *Journal of Materials Research and Technology*. 2023;27:585–599.  
<https://doi.org/10.1016/j.jmrt.2023.09.242>
  26. Otaru A.J., Auta M. Machine learning backpropagation network analysis of permeability, Forchheimer coefficient, and effective thermal conductivity of macroporous foam–fluid systems. *International Journal of Thermal Sciences*. 2024;201:109039.  
<https://doi.org/10.1016/j.ijthermalsci.2024.109039>
  27. Song S., Rong L., Dong K., Liu X., Le-Clech P., Shen Y. Pore-scale numerical study of intrinsic permeability for fluid flow through asymmetric ceramic microfiltration membranes. *Journal of Membrane Science*. 2022;642:119920. <https://doi.org/10.1016/j.memsci.2021.119920>

### Information about the Authors



### Сведения об авторах

**Vadim S. Shustov** – Cand. Sci. (Eng.), Senior Research Scientist at the Laboratory of Physical Chemistry of Surfaces and Ultrafine Powder Materials, Baykov Institute of Metallurgy and Materials Science of the Russian Academy of Sciences (IMET RAS)

 **ORCID:** 0000-0001-6395-3747

 **E-mail:** vshscience@mail.ru

**Viktor A. Zelensky** – Cand. Sci. (Phys.-Math.), Leading Researcher at the Laboratory of Physical Chemistry of Surfaces and Ultrafine Powder Materials, IMET RAS

 **ORCID:** 0000-0002-4441-9132

 **E-mail:** zelensky55@bk.ru

**Mikhail I. Alymov** – Dr. Sci. (Eng.), Corresponding Member of RAS, Head of the Laboratory of Physical Chemistry of Surfaces and Ultrafine Powder Materials, IMET RAS

 **ORCID:** 0000-0001-6147-5753

 **E-mail:** alymov@ism.ac.ru

**Alexey B. Ankudinov** – Senior Research Scientist at the Laboratory of Physical Chemistry of Surfaces and Ultrafine Powder Materials, IMET RAS

 **ORCID:** 0009-0002-1150-8515

 **E-mail:** a-58@bk.ru

**Alexey S. Ustyukhin** – Cand. Sci. (Eng.), Junior Research Scientist at the Laboratory of Physical Chemistry of Surfaces and Ultrafine Powder Materials, IMET RAS

 **ORCID:** 0000-0003-1578-4883

 **E-mail:** fcbneo@yandex.ru

**Вадим Сергеевич Шустов** – к.т.н., науч. сотрудник лаборатории физикохимии поверхности и ультрадисперсных порошковых материалов, Институт металлургии и материаловедения им. А.А. Байкова Российской академии наук (ИМЕТ РАН)

 **ORCID:** 0000-0001-6395-3747

 **E-mail:** vshscience@mail.ru

**Виктор Александрович Зеленский** – к.ф.-м.н., вед. науч. сотрудник лаборатории физикохимии поверхности и ультрадисперсных порошковых материалов, ИМЕТ РАН

 **ORCID:** 0000-0002-4441-9132

 **E-mail:** zelensky55@bk.ru

**Михаил Иванович Альмов** – д.т.н., чл.-корр. РАН, зав. лабораторией физикохимии поверхности и ультрадисперсных порошковых материалов, ИМЕТ РАН

 **ORCID:** 0000-0001-6147-5753

 **E-mail:** alymov@ism.ac.ru

**Алексей Борисович Анкудинов** – ст. науч. сотрудник лаборатории физикохимии поверхности и ультрадисперсных порошковых материалов, ИМЕТ РАН

 **ORCID:** 0009-0002-1150-8515

 **E-mail:** a-58@bk.ru

**Алексей Сергеевич Устюхин** – к.т.н., мл. науч. сотрудник лаборатории физикохимии поверхности и ультрадисперсных порошковых материалов, ИМЕТ РАН

 **ORCID:** 0000-0003-1578-4883

 **E-mail:** fcbneo@yandex.ru

### Contribution of the Authors



### Вклад авторов

**V. S. Shustov** – defined the purpose of the work, conducted experiments to determine permeability, participated in the discussion of the results, and wrote the article.

**V. A. Zelensky** – prepared mixtures and initial samples, participated in the discussion of the results, and editing the article.

**M. I. Alymov** – defined the purpose of the work and participated in the discussion of the results.

**A. B. Ankudinov** – determined the porosity of the samples and participated in the discussion of the results.

**A. S. Ustyukhin** – conducted electron microscopy of the samples' structure.

**В. С. Шустов** – определение цели работы, проведение экспериментов по определению проницаемости, участие в обсуждении результатов, написание текста статьи.

**В. А. Зеленский** – подготовка смесей и исходных образцов, участие в обсуждении результатов и редактировании статьи.

**М. И. Алымов** – определение цели работы, участие в обсуждении результатов.

**А. Б. Анкудинов** – определение пористости образцов, участие в обсуждении результатов.

**А. С. Устюхин** – проведение электронной микроскопии структуры образцов.

Received 05.08.2024

Revised 11.09.2024

Accepted 13.09.2024

Статья поступила 05.08.2024 г.

Доработана 11.09.2024 г.

Принята к публикации 13.09.2024 г.